

# **UV-VIS Spectral Analysis of Fluorescent Brightening Agents in Combination with Carrier Substances for Inkjet Based Substrate Whitepoint Simulations**

Daniel Bohn, Stefan Weber, Michael Dattner, Stefan Fehmer, Peter Urban

Keywords: fluorescent brightening agents, fluorescence, whitepoint, inkjet

## **Abstract**

In this study, colorimetric as well as chemical studies of commercially available fluorescent brightening agents (FBAs) are conducted. Thereby, special attention is given to polyethylene glycol (PEG) with varying molar masses, which is a known carrier for “boosting” and “activating” fluorescence and ethylene glycol (EG). While the colorimetric analysis focuses on printed laboratory FBA-inks containing liquid FBAs and in selected cases PEG, the chemical analysis is performed detached from the molecular environment “paper”.

It is shown, that the chain-length of PEG has a significant impact on the obtainable quantum yield and therefore emission intensity. Based on spectral analysis, it is concluded that PEG decreases the reaction rate of the isomerization reaction (due to a hindering of the twist of the C=C double bond) resulting in longer periods in which the excited state of the trans-isomer can exist. This leads to an increased amount of fluorescence from the excited trans-isomers. Hence, the obtained quantum yield is increased. Quantum yield increases from 33%  $Q_{eff}$  (in pure water) to 60% (in 30% PEG 1000) are reported.

## **Introduction**

One of the key goals in producing paper and cardboard in the print industry is to achieve a high whiteness degree. This is often realized by the addition of FBAs (Fluorescent Brightening Agents) to the paper pulp and coating (Champ, 2001). The heavy use of FBAs in production substrates, in contrast to proof-substrates that contain often a very limited amount of FBAs, result in serious difficulties in any

---

Bergische Universität Wuppertal

color management process, especially in terms of white point corrections.

In a preceding JPMTR-journal article, the authors of this study presented a method to achieve an illumination independent colorimetric and visual match between a single proof substrate and most production substrates. This has been accomplished by printing area coverage variable defined amounts of a liquid FBA using inkjet (Bohn, 2016). This preceding research will be briefly reviewed in the chapter “State of the scientific knowledge & resulting questions.”

Anyhow, the key to successfully implement this new type of whitepoint modification is the possibility to achieve an intense FBA-emission even with minor FBA-ink area coverages to e.g. not negatively affect the total ink volume of the used proof-substrate.

Therefore, this study focuses on the interaction of FBA-inks and carriers on a chemical level with special respect to observed quantum efficiencies of typical FBAs and carriers. Especially the influences of carrier chain lengths on the quantum efficiencies due to effects on the photo isomerization process of stilbene will be discussed in detail.

### **State of the scientific knowledge**

In this chapter a brief overview about fluorescence in general and relevant properties and mechanics of fluorophores of the type “stilbene” are given.

#### *Fluorescence in general*

Fluorescence is the emission of photons by molecules that have absorbed electromagnetic radiation. Thereby, emitted photons are typically of longer wavelength, and possess therefore a lower energy, than the absorbed radiation. With other words, the emission of photons by fluorescence molecules result in a red-shift. Such types of molecules are called “fluorophores”.

Thereby, many fluorophores absorb invisible UV-radiation and reemit the absorbed energy in the visible range of the spectra; hence, the fluorescence effect becomes visible to the human eye.

Fluorophores cease to glow immediately after the radiation source stops, unlike phosphorescence, whereby photons are emitted for a significant longer time after (Sauer, 2011).

#### *FBAs and Carriers in the print- and media Industry*

In practice, most used fluorophores in the print- and paper industry are based upon stilbene-derivates, of the type “4,4'-Diamino-2,2'-stilbene-X-sulfonic acid”.

Thereby, the X represents the sulfonation-degree of the molecule, which can be di-, tetra- or hexa-sulfonated. The number of sulfo-groups mainly determines the solubility of the molecules in water.

- Diaminostilbene-disulfonated FBAs have two sulfonic groups. The two other substituents could be hydrophilic groups. These FBAs show a very good affinity to cellulose, but a limited solubility and are mostly used in the wet-end (Holik, 2006).
- The most commonly used FBA is of the tetra-sulfonated type. Tetra sulfonated FBAs are a versatile substance because of their medium affinity and good solubility. They can be used in most stages of papermaking: wet-end, size-press and coating (Holik, 2006).
- Hexa-sulfonated FBAs are especially used in coatings, where high brightness is required (Holik, 2006).

*Please note, most commercially available FBAs are substituted with additional functional groups to achieve special properties such as acid resistance or to gain a defined red shift.*

Anyhow, the performance of these FBAs has been subject to intense research on a practical scale, mainly with focus on empirical determination of the highest whiteness gains possible by changing parameters, such as the concentration of the FBA or the addition of known carrier substance.

Thereby, carrier substances are molecules that are known to “intensify” or even “enable” fluorescence on an empirical scale. Used and examined carrier substances are for example polyethylene glycol (PEG), methyl cellulose (MC) or polyvinyl alcohol (PVA), with in each case differing molar masses (and therewith chain lengths of the molecule) and hydrolysis degrees (Blum, 2002).

Some studies show that the type of carrier substance, the used concentration, the actual hydrolysis degree or even the point of time at which the carrier has been added to paper pulp during paper production and lead to individual effects. Thereby, all examinations have been done for actual paper compositions and not detached from the molecular environment “paper” (e.g. Blum, 2002). Therefore, all these studies are to be classified as empirical.

Anyhow, Paltakari (2009) and Blum (2002) postulated two theories about the operating principle of carriers. While Paltakari postulates that carrier substances and FBAs form “some kind of complex”, Blum suggests that carrier enable a monomolecular distribution of the FBAs in one layer on paper substrates (Paltakari, 2009) (Blum, 2002). In both cases, no further explanations are provided.

## Fluorescence of stilbene

The Jablonski diagram is convenient for visualizing possible processes like photon absorption, internal conversion (IC), intersystem crossing (ISC), phosphorescence, delayed fluorescence, and triplet – triplet transitions in a simple way. Furthermore, fluorescence of stilbene can be visualized easily using Jablonski diagrams as shown in figure 1. The singlet electronic states are denoted by  $S_0$ ,  $S_1$ , and  $S_2$ ... Please note that absorption is very fast ( $\approx 10^{-15}$ s) with respect to all other processes. The vertical arrows correspond to absorption that starts from the (lowest) vibrational energy level of the  $S_0$  ground-state, because the majority of molecules are at room temperature in this level. Absorption of a photon by a trans-stilbene molecule (cf. chapter “photo isomerization”) can excite the molecule to one of the vibrational levels of  $S_1$  or  $S_2$  depending on the actual energy of excitation. Thereby, for wavelengths between 250 and 310nm, trans-isomer stilbene solved in ethanol are excited from the ground state  $S_0$  to the excited singlet state  $S_2(v_0, v_1, \dots, v_n)$ . Due to vibrational relaxation (VR) of the molecule  $S_2(v_0)$  is reached. From this stage, the molecule undergoes an IC to  $S_1(v_x)$ . This higher vibrational level in  $S_1$ , undergoes VR to  $S_1(v_0)$ .

This higher vibrational level in  $S_1$ , undergoes VR to  $S_1(v_0)$ . From this excited singlet state fluorescence can occur, i.e. the molecule reaches  $S_0(v_0, v_1, \dots, v_n)$  and a photon is emitted containing the corresponding energy difference.

For wavelength of 310-370nm the molecule is excited from  $S_0$  to  $S_1(v_0, v_1, \dots, v_n)$ . Again, because of vibrational relaxation energy is reduced until  $S_1(v_0)$  is reached. From this particular singlet state photons are emitted until  $S_0(v_0, v_1, \dots, v_n)$  is reached.

Because of the STOKES shift the emitted energy for  $S_1 \rightarrow S_0$  is always of lower energy and shows therefore a red-shift (cf. Gispert, 2008).

Because of KASHA's rule, the underlying processes lead to a certain mirror image of the absorption spectra (the part that leads to a  $S_0 \rightarrow S_1$  transition) and the emission spectra (Kasha, 1950).

Further, detailed information about the Jablonski diagram in terms of fluorescence are discussed and explained by e.g. Sauer (2011).

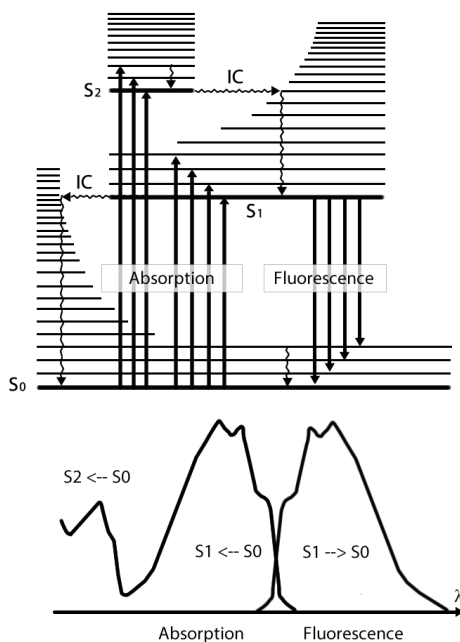


**Figure 1:** Jablonski diagram of stilbene (absorption and fluorescence). Straight arrows represent radiative processes, whereas wavy arrows stand for non-radiative processes. The orientation of the arrows directly gives information if an absorption is present (up-arrow) or an emission takes place (down-arrow)

### Quantum Yield

One major parameter for characterizing as well as determining whether an FBA is suitable for practical applications or not, is the quantum yield.

The fluorescence quantum yield  $\Phi_F$  is the fraction of excited molecules that return to the ground state S<sub>0</sub> by emitting photons:

$$\Phi_F = \frac{k_r^S}{k_r^S + k_{nr}^S}$$

*Formula 1: Quantum yield*

with:

- $k_r^S$  as the rate constant of the fluorescence
- $k_{nr}^S$  as the overall non-radiative rate constant
- $\Phi_F$  as the quantum yield

In other words, the fluorescence quantum yield is the ratio of the number of emitted photons (over the whole duration of the decay) to the number of absorbed photons, hence the qualifier is called “quantum”. Owing to the Stoke’s shift, fluorescence yield expressed in terms of energy is always lower than the energy in total (Sauer, 2011).

If every photon absorbed results in a photon emitted, the maximum fluorescence quantum yield is 1.0. Substances with quantum yields of 0.10 are still considered fluorescent.

### Parameters affecting Florescence

Several parameters are known to influence fluorescence in terms of observed quantum yields as well as the wavelength and characteristics of fluorescent emission ( $\rightarrow$  emission shape). Possible parameters are polarity of the solvent, available hydrogen bonds, pH-value of the solvent, pressure, viscosity, temperature, presence of quenchers, electric potential and ions.

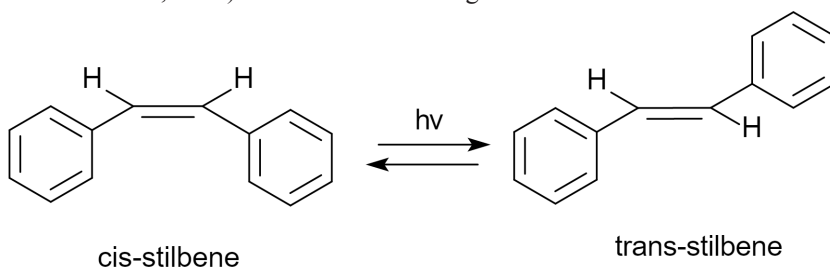
E.g., the viscosity of a solvent affects directly the obtainable quantum yield: A higher viscosity leads typically to an increased quantum yield. This relation is described by the FÖRSTER-HOFFMANN law (cf. formula 3).

In the context of this study, the parameter “viscosity” is considered with special attention (cf. chapter “Quantum Yield of the tetra-based FBA in dependency of different PEG- concentrations and -molar masses”).

### Photo isomerization of stilbene

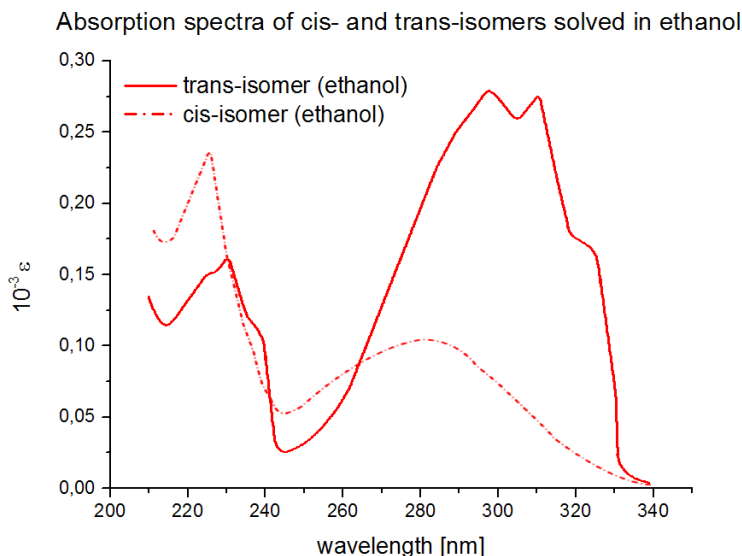
In chemistry, photo isomerization in general is molecular behavior in which structural changes between isomers are caused by photoexcitation. Both, reversible and irreversible isomerization reactions exist. However, photo isomerization is typically a reversible process as it is found for stilbene.

A simple functional entity, allowing for two different conformations, is the C=C double bond as it is found in the stilbene base structure as it is used in the research conducted for this paper. Based on the arrangement of the two largest ligands, a trans-isomer where both ligands are on opposite sides of the double bond, and a cis-isomer where both ligands are on the same side of the double bond, can be realized (Schmidt-Weber, 2008). Both are shown in figure 2.



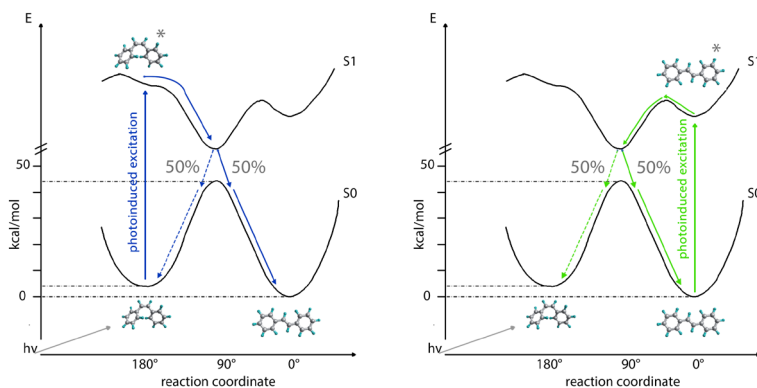
*Figure 2: Photon induced photo isomerization of stilbene*

Figure 3 shows the absorption spectra of both stilbene isomers, if solved in ethanol (cf. Beale, 1953). It can be seen that a common absorption minimum can be found at 245nm, while the absorption maxima between the cis- and the trans isomer differ significantly (cis-isomer: 280nm; trans-isomer: 305nm). Furthermore, the absorption of the trans-isomer in this wavelength region is much stronger, compared to the absorption of the cis-isomer.



**Figure 3:** Absorption spectra of the cis- and the trans-isomer solved in ethanol. Differences can be found especially in the wavelength region between 280nm and 340nm (following Beale, 1953).

Abrash and coworkers (2009) elaborated the corresponding energy diagram for the photoreactions of the stilbene isomers based upon the direct excitation into the  $S_1$  state (cf. Abrash, 2009). Figure 4 show several possible pathways for structural changes of the cis- and for the trans-isomer form respectively (following Abrash, 2009).



**Figure 4:** Energy diagram for conversion between stilbene isomers for a cis-isomer initiated isomerization (left) and a trans-isomer initiated isomerization (right)

Thereby, figure 4 (left) shows the pathway of a cis-isomer if excited into the excited singlet state S<sub>1</sub>. Because of this excitation the photo isomerization is initiated and leads to a change of reaction coordinate (abscissa in figure 4) with regards to the C=C double bonds angle  $\Theta$  (cf. figure 5). Following the reaction coordinate, the S<sub>1</sub>-potential is dropping until an energy of 50 kcal/mol is reached. At this point, the cis isomer relaxes back to the ground state S<sub>0</sub> with a 50% - 50% probability of further existing in the cis- or the trans-configuration respectively. Thereby, the lifetime of the excited cis state is 1ps (Todd, 1998). During this period the isomer is able to emit photons, but mainly at the same wavelength as it has been excited with (absorption = emission).

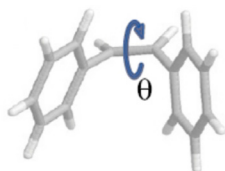


*Figure 5: Rotation coordinate  $\Theta$  of the C=C double bond of a stilbene molecule*

In contrast, figure 4 (right) shows the pathway of a trans-isomer if excited to the excited singlet state S<sub>1</sub>. Again, because of excitation, the photo isomerization is initiated and leads to a change of reaction coordinate with regards to the C=C double bonds angle  $\Theta$  (cf. figure 4 (right)). Following the reaction coordinate, the S<sub>1</sub>-potential is dropping again until an energy of 50 kcal/mol has been reached. At this point, the trans-isomer relaxes back to the ground state S<sub>0</sub> with a 50% - 50% probability of further existing either in the cis- or the trans-configuration. The main difference is the much longer lifetime of the trans-isomer, which has been determined to be 70ps long (Todd, 1998). The reason for the longer period arises from a local maximum of the potential curve, as it is shown in figure 4 (right). Again, during this period, the isomer is able to emit photons. Thereby, the trans-isomer emits at longer wavelengths (red-shift), what we perceive as fluorescence. Because of the much longer period in which the trans-isomer exists, more photons are emitted from the excited state. Another important implication of the extended lifetime is that more trans-isomers may exist since the photo isomerization is a continuous process.

## Methods

*This chapter is split into methods that have been used for colorimetric studies and methods, as well as procedures, that have been utilized for chemical studies*

### Colorimetric studies

For all colorimetric studies, a laboratory UV-VIS-Spectrophotometer of the company Tec5 GmbH with a spectral range of 250-780nm and a spectral resolution of 1nm in combination with a 200-Watt Xenon-high pressure light-source has been



used. The readings have been done using a 45/0-degree measurement geometry. Furthermore, several UV-Cut filter have been used to fully or partially suppress the excitation of FBAs that are applied to substrates.

Utilizing the principle of printing liquid FBAs using inkjet (cf. Bohn, 2016), three FBAs and (poly-)ethylene glycol ((P)EG) acting as a carrier with differing average molar masses have been applied (cf. table 1) to three (mostly) un-brightened substrates (cf. table 3).

Chemical name	Short name	Molecular mass [g/mol]
Di-sulfonated diamino-stilbene acid derivative	di-type	1036.57
Tetra-sulfonated diamino-stilbene acid derivative	tetra-type	1165.05
Hexa-sulfonated diamino-stilbene acid derivative	hexa-type	1513.00
Polyethylene glycol	PEG	200, 400, 1000, 2000 (average)
Ethylene glycol	EG	62.07

**Table 1:** Overview of used Fluorescent Brightening Agents and their relevant properties

Name	Manufacture	Grammage [g/m <sup>2</sup> ]	FBA	Surface	White point (MI)		
					L*	a*	b*
ProNatur	unknown	200	non	Uncoated, mate	99.31	-0.34	1.65
GMG SemiMatt	GMG	220	non	Coated, semi-mate	97.16	-0.68	-2.55
EFI BestXpress	EFI	250	non	Coated, semi-mate	96.38	0.24	-2.82

**Table 2:** Used substrates with relevant parameters

Sample number	Used FBA	Concentration [%]	Used Carrier	Carrier [%]	Water [%]
<i>Without Carrier</i>					
1-t	tetra-type	0.05	non	0	99.95
2-t	tetra-type	0.2	non	0	99.8
3-t	tetra-type	0.8	non	0	99.2
4-t	tetra-type	3.2	non	0	96.8
5-t	tetra-type	6.4	non	0	93.6
6-t	tetra-type	20	non	0	80
<i>With Carrier</i>					
4-t-1	tetra-type	3.2	PEG 1000	1	95.8
4-t-2	tetra-type	3.2	PEG 1000	2	94.8
4-t-3	tetra-type	3.2	PEG 1000	4	92.8
4-t-4	tetra-type	3.2	PEG 1000	8	88.8
20-t-1	tetra-type	20	PEG 1000	1	79
20-t-2	tetra-type	20	PEG 1000	2	78
20-t-3	tetra-type	20	PEG 1000	4	76
20-t-4	tetra-type	20	PEG 1000	8	72

**Table 3:** Overview about printed FBA & Carrier combinations as well as concentration variations

### Chemical studies

Bohn already showed that the molecular environment “substrate” strongly interacts with FBA-inks (Bohn, 2016). Because UV-VIS-reflectance spectrometer based readings (cf. chapter “colorimetric considerations”) do not allow readings of the absorption, excitation & emission behavior of FBAs and carries *independently* from substrates UV-VIS-measurements on a chemical level are needed.

For that reason, to fully understand the occurring interactions of the FBA- and carrier-molecules, absorption spectra of all FBAs and carriers (cf. table 3) have been acquired in an aqueous solution by utilizing a UV-Vis-spectrometer (device name: Carry 50; company: Agilent Technologies; spectral range: 200-900nm). Thereby, this type of spectrometer gathers data from liquids based on transmission readings (in contrast to the UV-Vis-reflectance spectrometer as it is used for substrate measurements (cf. chapter “colorimetric studies).

Next, a fluorescence spectrophotometer (device name: Cary Eclipse; company: Agilent Technologies; spectral range: 200-900nm) is utilized to gain spectral emission and excitation readings of all FBAs with and without carrier dissolved in an aqueous solution.

This way, substrate related effects are avoided and a reliable base is given to study previously observed effects, like greening and substrate depending emission intensity differences on a chemical founded level.

These readings are used to calculate fluorescent quantum yields of isolated FBAs in pure water and with several ethylene glycol and polyethylene glycols and concentrations acting as solvents. It is important do understand that, next to (P)EG, other substances are known to act as a carrier. Anyhow, (P)EG shows no absorption at the excitation wavelength of interest (340nm) nor at wavelengths showing emissions (380-550nm), even for concentrations up to 30%.

The quantum yield of the analyzed FBAs is calculated by utilizing Formula 2. This formula is an easy and commonly accepted way to determine the quantum yield of unknown substances. Thereby, this method relays on a fluorescence standard with a known quantum yield. For this study the substance anthracene (CAS: 120-12-7), dissolved in ethanol, is utilized as a fluorescence standard. Anthracene is known to possess an average quantum yield of 0.27 in ethanol (Melhuish, 1961). Furthermore, the absorption and emission spectra of anthracene is suitable for the chosen excitation wavelength of 340nm, which has been selected for all excitation analysis in this study. The absorption and emission spectra of anthracene is shown in figure 6.

$$\Phi_X = \Phi_{ST} \left( \frac{\text{Grad}_X}{\text{Grad}_{ST}} \right) \left( \frac{\eta_X^2}{\eta_{ST}^2} \right)$$

*Formula 2: Used formula to determine quantum yields*

With

- $\Phi_X$  as the quantum yield of an unknown substance
- $\Phi_{ST}$  as the known quantum yield of a fluorescence standard
- $Grad_x$  as the linear gradient of the unknown substance
- $Grad_{ST}$  as the linear gradient of the fluorescence standard
- $\eta^2_x$  as the squared refraction index of the solvent, which has been used to solve the unknown substance
- $\eta^2_{ST}$  as the squared refraction index of the solvent, which has been used to solve the fluorescence standard

*Please note I:* The linear gradient can be calculated from different absorption levels (Absorption  $\leq 0.1$ ) that are plotted against the integrated emission.

*Please note II:* Both, the FBAs as well as the fluorescence standard have been diluted until an absorption max of 0.1 had been reached to avoid non-linear effects like inner filter effects.

A full description of the for this study utilized approach to calculate the quantum yield is described by (Horiba, 2017).

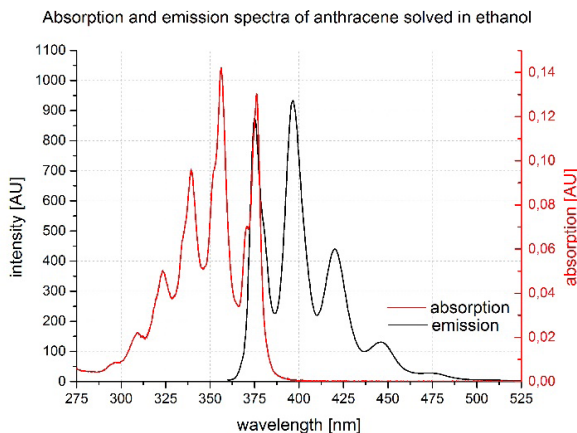


**Figure 6:** Absorption and emission spectra for anthracene solved in ethanol for an absorption of 0.1 at 340nm

Additionally, obtained spectral absorption and emission readings are used for further analysis.

Finally, the viscosity of all solvents has been determined by utilizing a rheometer, since increasing viscosities are known to have an effect on the obtained quantum yield (cf. chapter “Influences on fluorescence”).

## Results

This chapter is divided in colorimetric based considerations regarding printed FBA-s using inkjet and chemical based considerations of FBAs in the liquid state

### Colorimetric Consideration

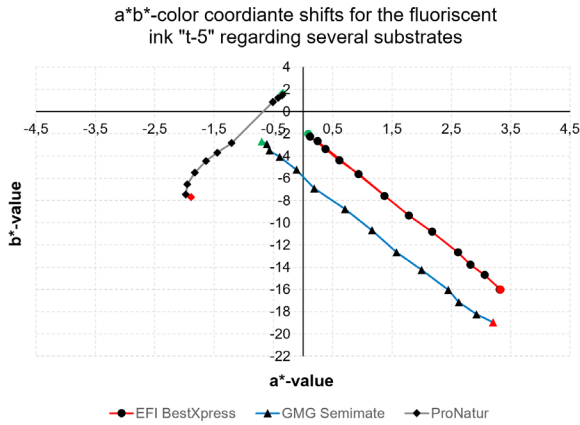
#### *Substrate specific comparison for a single FBA-type & -concentration*

Figure 7 shows the  $a^* b^*$ -color coordinates for the FBA-ink “t-5” (cf. table 3) with area coverages starting from 0% (whitepoint of the substrate) up to 100% in 10% steps. Thereby, the green mark equals a 0% area coverage and the red mark equals a 100% area coverage in each case.

In the case of the substrate “GMG-Semimate” a strong negative increase of the  $b^*$ -value ( $b^*_{0\%-AC} = -2.5 \rightarrow b^*_{100\%-AC} = -19.1$ , with AC as the area coverage of the applied FBA) can be observed, while the  $a^*$ -value only slightly increases ( $a^*_{0\%-AC} = -0.85 \rightarrow a^*_{100\%-AC} = 3.1$ ). Thereby, the  $a^* b^*$ -shift shows a linear behavior for all area coverages. Please note that this linear behavior is known to be a typical FBA-emission behavior without any greening.

The substrate “BestXpress” behaves comparable to the substrate “GMG-Semimate”. Only the whitepoint differs right from the beginning (GMG-Semimate:  $a^* : -0.85$ ;  $b^* : -2.5$  / Best-Xpress:  $a^* : 0.1$ ;  $b^* : -1$ ). Apart from that, the same linear  $a^* b^*$ -behavior is observed.

In the case of the substrate “ProNatur” a moderate increase of the negative  $b^*$ -value ( $b^*_{0\%-AC} = 2 \rightarrow b^*_{100\%-AC} = -8.3$ ) is found, while the  $a^*$  value shows a significant decrease ( $a^*_{0\%-AC} = -0.43 \rightarrow a^*_{100\%-AC} = -1.9$ ). Thereby, the  $a^* b^*$ -shift shows a non-linear behavior for high area coverages (90% & 100%). Divergent from the already discussed substrates, this papers whitepoint shifts towards coordinates of the Lab-system that are associated with the color impression “green”. This can be interpreted as significant greening.



**Figure 7:** *a\*b\*-color coordinate shifts of a tetra-based FBA-ink (6.4% concentration) for area coverages of 0% - 100% regarding three differing substrates without carrier*

To outline these effects, figure 8 shows the spectral response of all three substrates once with an area coverage of 0% (actual paper whitepoint) and once with 100% FBA-ink area coverage.

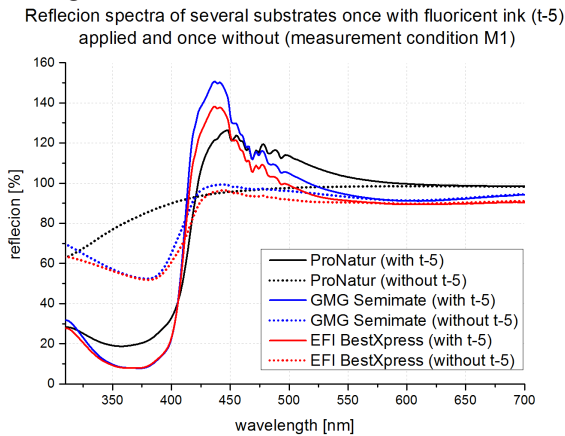


**Figure 8:** *Reflectance spectra of three substrates once with FBA-ink (type: t-5; 100% area coverage) and once without (0% area coverage) applied to three substrates and once without (measurement condition: M1)*

In conclusion, it can be argued that the molecular environment “paper” has a significant influence on the performance of applied FBAs using inkjet.

### Influence of different FBA-concentrations

Figure 9 shows the influence of several FBA-concentrations (0.8%, 3.2%, 6.4% & 20%) on the  $a^*b^*$ -color coordinates for several area coverages. For concentrations of 0.8%, 3.2% & 6.4% an increase of the negative  $b^*$ -value is observed and therefore an increase of emission. Thereby, the  $a^*$ -value is slightly increasing in a comparable way. Anyhow, for a concentration of 20%, the  $b^*$ -value is lower than for the 6.4% concentration. Furthermore, the  $a^*$ -value is in comparison significantly decreased. This leads to a significant greening. In conclusion, an increase of absorption leads to intensified blue emissions until a certain point is reached and the blue emission becomes greenish. This may occur because of inner filter effects or quenching.

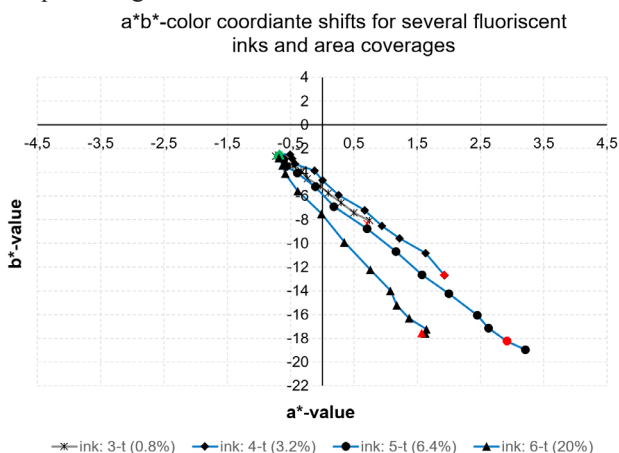


**Figure 9:**  $a^*b^*$ -color coordinate shifts of several tetra-based FBA-inks varying in their concentration (0.8%, 3.6%, 6.4% & 20%) for area coverages of 0% - 100% without carrier regarding the substrate "GMG Semimate"

Figure 10 shows the influence of polyethylene glycol with an average molar mass of 1000 g/mol in a concentration of 8% added to 3.2% & 20%-FBA-inks. For the 3.2%-ink, the  $b^*$ -value is nearly doubled from -12.7 to -24.01. Therefore, the obtained blue emission is also nearly doubled. For the 20%-ink, the greening is prevented. Anyhow, the  $b^*$ -value is decreases from -17.9 to -16.

In conclusion, it is shown that the addition of PEG enables stronger fluorescent emissions on substrates while greening is prevented. Anyhow, the presented colorimetric analysis does not allow conclusions about the way PEG interacts with FBAs. Because substrates are complex, in terms of their molecular structure, it is difficult to line up interpretations of observed effects.

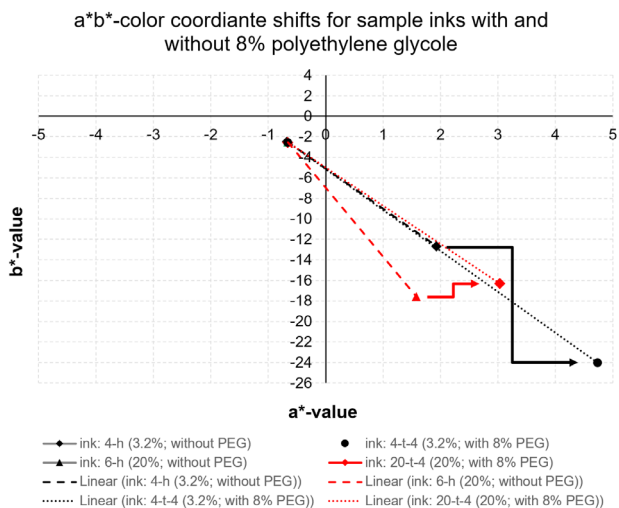


**Figure 10:** *a\*b\*-color coordinate shifts induced by the FBA-inks 4-h, 6-h (without carrier) 4-t-4 and 20-t-4 (with carrier) regarding the substrate “GMG Semimate”*

Hence, in the next chapter “Chemical Considerations” FBAs and Carriers are studied detached from the molecular environment paper in the liquid state.

### Chemical Considerations

Quantum Yield and spectral analysis of used FBAs without carrier in solution

Figure 12 shows the obtained absorption values of all FBAs & anthracene plotted against the integrated emission intensity for an excitation wavelength of 340nm. It can be seen, that all measurements of a diluting series show linear gradients with very good correlation coefficients ( $R^2$ ) of 0.9967 up to 0.9902. Furthermore, all gradients run through the zero point of the diagram. This is a strong evidence that no impurities of the solutions distort the obtained quantum yields.

The obtained values are used to calculate individual quantum yields (cf. figure 11) by utilizing formula 2.

Visualisation of the obtained integrated emission values vs. measured absorptions at 340nm for several fluophor samples and one fluorescence standard (Anthracene)

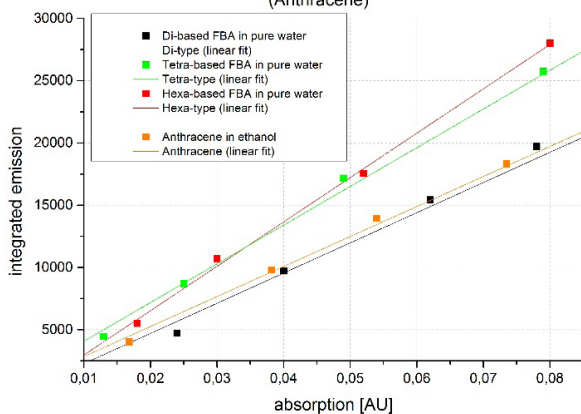


**Figure 11:** Visualization of obtained emission values plotted against measured absorptions at 340nm for the FBAs “di-type”, “tetra-type” and “hexa-type”. The linear dependency obtained for each sample-series show very good  $R^2$ -values. Furthermore, all grades run through the 0-point of the diagram, indicating that no impurities or measurement errors have compromised the results.

Name	Used solvent	Average molar mass [g·mol <sup>-1</sup> ]	Quantum yield $\phi$ [%]
Di-type	H <sub>2</sub> O	1036.57	26%
Tetra-type	H <sub>2</sub> O	1165.05	33%
Hexa-type	H <sub>2</sub> O	1513.00	38%
Anthracene	Ethanol	178.23	27%

**Table 4:** Details about used FBAs and the fluorescence standard “anthracene” with obtained quantum yields

For the FBA “tetra-type” a quantum yield of 0.33 was found, while the FBA “hexa-type” shows a slightly higher quantum yield of 0.38. The FBA “di-type” shows the lowest quantum yield of 0.26.

Figure 12 shows the normalized absorption and emission spectra of all three FBAs.



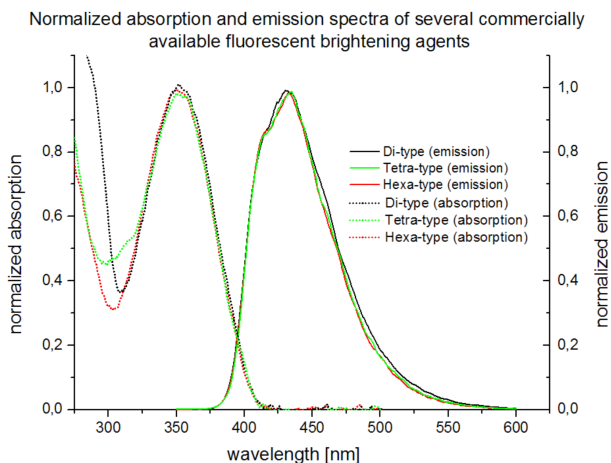


**Figure 12:** Normalized absorption and emission spectra of several FBAs solved in H<sub>2</sub>O. Common emission maxima at 435nm and common absorption maxima at 350nm are obtained. Differences in local minima are found in the range of 275-325nm

It can be seen, that the normalized emission spectra of all three FBAs (di-, tetra- and hexa-sulphonated) correlate very well. This is also true for the main absorption at 350nm, which is very relevant for practical applications in the print and paper industry. Only the secondary absorptions (for wavelengths  $\leq 325$ nm) show significant differences.

It can be stated that the number of sulphonic-groups do not affect the relevant absorption wavelength area (320-420nm) as well as the shape of the emission spectra (380 – 570nm). Furthermore, it can be derived that most likely existing functional groups, that are able to change the wavelength of absorption and emission, are present in a comparable manner in all three types of FBA. This assumption is derived from the molar mass of the diaminostilbene base molecule and the molar masses of the commercially available FBAs. The assumption that functional groups are in fact influencing e.g. the emission wavelength is derived from the fact that the base stilbene shows absorption and emission wavelengths of lower energy (cf. figure 3).

#### *Quantum Yield of the tetra-based FBA in dependency of different PEG-concentrations and -molar masses*

So far, the FBAs “di-type”, “tetra-type” & “hexa-type” have been studied, if dissolved in pure water acting as a solvent. In this chapter the tetra-based FBA is examined with regard to its interaction with (P)EG, which is known to be a suitable carrier to “activate” and “intensify” the emission. The used molar masses of (P)EG are presented in table 3. in chapter “Methods”.

Table 5 shows the obtained quantum yields of the tetra based FBA for several solutions which are composed out of poly- (ethylene glycol) with different molar masses (and therefore different chain lengths) and concentrations. The rest of the solution is substituted with pure water in each case. Thereby, the prepared combinations of (P)EG and water are acting as solvents.

Additionally, the measured solution specific refractive indexes as well as measured viscosity values are shown.

Name	Added substance	Average molar mass [g·mol <sup>-1</sup> ]	(P)EG [%]	H <sub>2</sub> O [%]	Viscosity [mPa·s <sup>-1</sup> ]	Quantum yield	Refraction index
EG 10%	Ethylene glycol	62.07	10	90	1.34	0.373	1.347
EG 30%	Ethylene glycol	62.07	30	70	2.64	0.441	1.381
EG 50%	Ethylene glycol	62.07	50	50	3.95	0.496	1.401
EG 100%	Ethylene glycol	62.07	100	0	10.1	0.60	1.451
PEG 200, 2.5%	Polyethylene glycol	200	2.5	97.5	1.08	0.374	1.335
PEG 200, 5%	Polyethylene glycol	200	5	95	1.27	0.417	1.338
PEG 200, 10%	Polyethylene glycol	200	10	90	1.66	0.511	1.342
PEG 200, 30%	Polyethylene glycol	200	30	70	4.08	0.580	1.377
PEG 400, 2.5%	Polyethylene glycol	400	2.5	97.5	1.25	0.436	1.336
PEG 400, 5%	Polyethylene glycol	400	5	95	1.4	0.486	1.334
PEG 400, 10%	Polyethylene glycol	400	10	90	1.75	0.548	1.344
PEG 400, 30%	Polyethylene glycol	400	30	70	5.1	0.607	1.376
PEG 1000, 2.5%	Polyethylene glycol	1000	2.5	97.5	1.56	0.535	1.339
PEG 1000, 10%	Polyethylene glycol	1000	10	90	2.04	0.594	1.345
PEG 1000, 30%	Polyethylene glycol	1000	30	70	8.32	0.599	1.391

**Table 5:** Obtained viscosities, refraction indexes and quantum yields for several (P)EG solutions

Please note, that PEG and EG have been chosen for further analysis since all variants of this substance show no absorption at the excitation wavelength at 340nm and in the wavelength area 380- 570 where the emission takes place. Hence, direct comparisons of the obtained quantum yields become possible.

Figure 13 shows the logarithmically plotted quantum yield against the logarithmically plotted viscosity for all solvents in combination with the tetra-based FBA (5-t).

For the solvents based upon the substance ethylene glycol (EG) with concentrations of 10%, 30%, 50% and 100% a linear dependency can be identified. The obtained quantum yield is growing for increasing viscosities. This behavior is in accordance with the FÖRSTER-HOFFMANN law (cf. formula 2).

$$\log \Phi = C + x \log \eta$$

*Formula 3: Förster-Hoffmann law*

with:

$\Phi$  as the quantum yield

$\eta$  as the viscosity of the solvent

$C$  as a temperature dependent constant

$x$  as a substance specific constant

Influence of the viscosity and the carrier chain length on the quantum efficiency

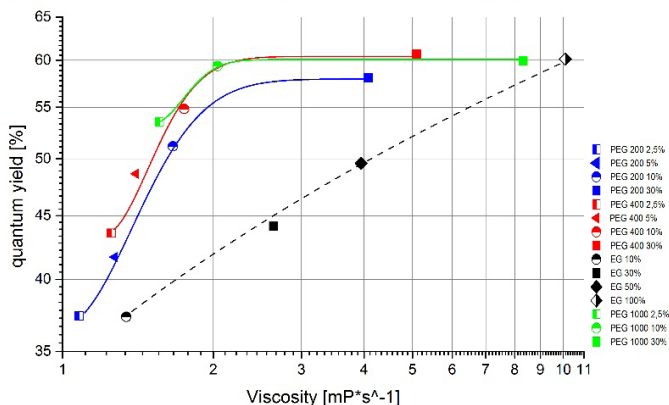


**Figure 13:** Influence of the solvents viscosity and carrier chain-lengths on the quantum yield

For all other solvents that base on PEG (concentration >10%) this law *seems* to fail. E.g., in the case of PEG 200 with an average molar mass of 200g/mol no linear dependency can be observed for concentrations of 2.5%, 5%, 10% and 30%. In particular, low concentrations of PEG 200, PEG 400 and PEG 1000, and therefore low viscosity changes (PEG 200 2.5% → 1.1mPa → PEG 200 5% → 1.2mPa → PEG 200 10% → 1.4mPa), result into dramatic higher quantum yield gains compared to EG solutions (10% → 1.06 mPa). A comparable behavior can be observed for PEG 400 & PEG 1000 based solvents. Anyhow, if only moderate high concentrations of PEG are used (e.g. PEG 200 2.5%, 5% and 10%) a linear behavior can be identified (cf. figure 14).

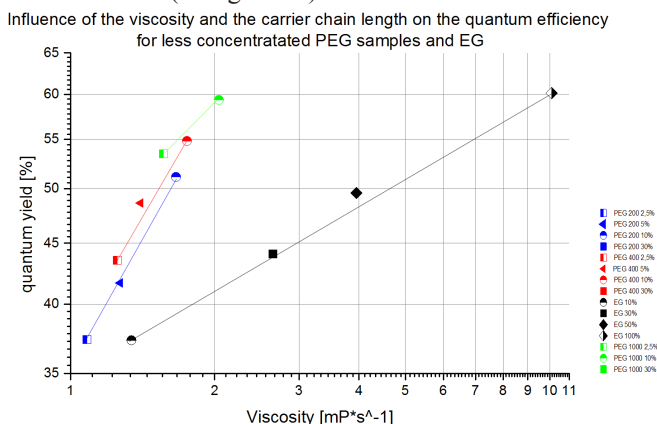


**Figure 14:** Influence of the solvents viscosity and carrier chain-lengths on the quantum yield for selected concentrations of EG and PEG in H<sub>2</sub>O. A linear dependency is found in accordance to the “Förster-Hoffmann-Law”

In conclusion, it can be assumed that this behavior results from a maximum quantum yield that can be achieved by slowing down the inversion reaction (C=C double bond twist). Other non-fluorescent deactivation reactions are not affected, so the quantum yield can not be increased beyond this value (cf. figure 5). Therefore, the period in which especially the trans-isomer exists is extended. Anyhow, because the only difference between all solvents can be found in the chain length of the molecules (which only moderately increases the viscosity) this parameter seems to influence massively the obtainable quantum yield even for low concentrations of PEG compared to EG.

To outline this behavior figure 15 shows a reduced dataset. Again, all EG based solvents with 10%, 30%, 50% & 100% are shown, while only the 10% concentration variant of the PEG 200, PEG 400 and PEG 1000 solvents are plotted. Even the 30% EG solution, which shows a comparable low viscosity of 2.64 compared to the viscosities of 10% PEG 200 (viscosity: 1.66), PEG 400 (viscosity: 1.75) & PEG 1000 (viscosity: 2.04), shows a significant lower quantum yield of 37% compared to the quantum yields obtained from the other solutions (PEG 200 10%:  $Q_{\text{eff}}$ : 0.551, PEG 400 10%:  $Q_{\text{eff}}$ : 0.548, PEG 1000 10%:  $Q_{\text{eff}}$ : 0.594).

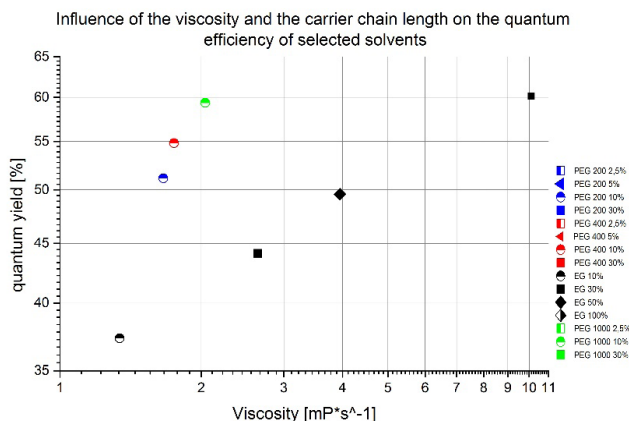


**Figure 15:** Influence of the solvents viscosity and carrier chain-lengths on the quantum yield for selected chain-lengths of PEG in comparison with EG in H<sub>2</sub>O. The parameter chain length leads to higher quantum yields for lower viscosities.

These data indicate that not only the viscosity affects the quantum yield but especially the chain length of the molecules, which can be interpreted as a substance specific parameter, as it is considered by the FÖRSTER-HOFFMANN law. One possible explanation is that the chains lead to a certain “physical” hindering of the isomerization. This effect is possibly intensified due to in one another cross-linked chains, increasing the physical boundary of the C=C double bond twist of the isomerization and thus reduces the reaction speed of the isomerization itself. With figure 4 in mind, it can be assumed that the lifetime of the excited trans-isomer is further extended by this effect (viscosity and chains), leading to a higher ratio of the fluorescent trans-isomers compared to the less fluorescent cis-isomers. This in conclusion results in an increased quantum yield compared to non-chained-molecules such as ethylene glycol.

To give further proof, a spectral analysis of the absorption spectra of the tetra-based FBA shows a significant red-shift for all 30% PEG-solutions compared to pure water (10nm shift) and the EG-based solutions with concentrations of 50% and 100% (4nm shift) (not shown).

As shown in the chapter “State of the scientific knowledge” the absorption spectra of the cis- and the trans-isomers differ significantly (cf. figure 3). More precisely, the trans-isomers absorption shows a significant red-shift in the wavelength region of 290-340nm compared to the cis-molecules absorption (cf. figure 16).

If these spectra are compared with the absorption spectra of the tetra-type FBA once solved in pure water and once solved in 30% PEG 1000, it can be seen, that the local absorption minimum of 310nm remains the same, while the peak at 345nm (pure water) shifts to 355nm (30% PEG 1000) (cf. figure 16).

Against this background, it can be assumed that the shift of wavelength results from a higher ratio of trans-isomers that have a higher fluorescence quantum yield in PEG and are therefore changing the isomer ratio, benefiting the trans-isomer. As already shown (cf. figure 13), this effect occurs also of increasing viscosities but much less distinct compared to solutions containing PEG (and therefore longer chains). In conclusion, this gives another indication that the quantum yield is increasing due to higher numbers of trans-isomers that are excited for an extended time-frame.

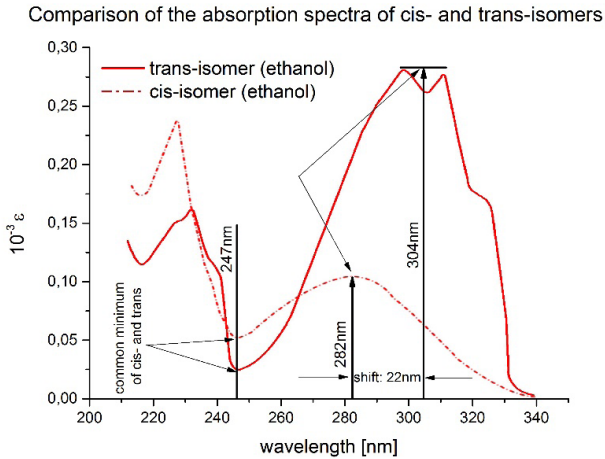


**Figure 16:** Absorption spectra of cis- and trans-isomers solved in ethanol

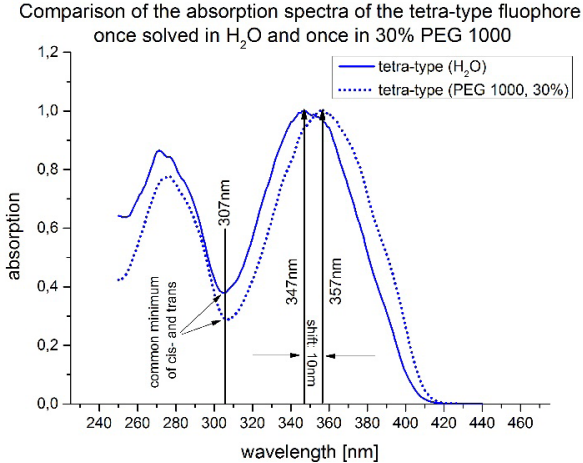


**Figure 17:** Absorption spectra of the tetra-based FBA once solved in pure water and once in 30% PEG 1000

Figure 18 shows the absorption as well as the emission spectra of the tetra-based FBA once solved in PEG 1000 (30%) and once solved in pure water. Next to the already shown red-shift of the absorption, a blue-shift of the emission is obtained. Furthermore, the blue-shifted emission (tetra-FBA in 30% PEG 1000) shows a “double peak”, if compared to the FBA solved in pure water. This double peak is also found for the pure trans-isomer (cf. Figure 16). Hence, the “mirror-rule” applies very well.

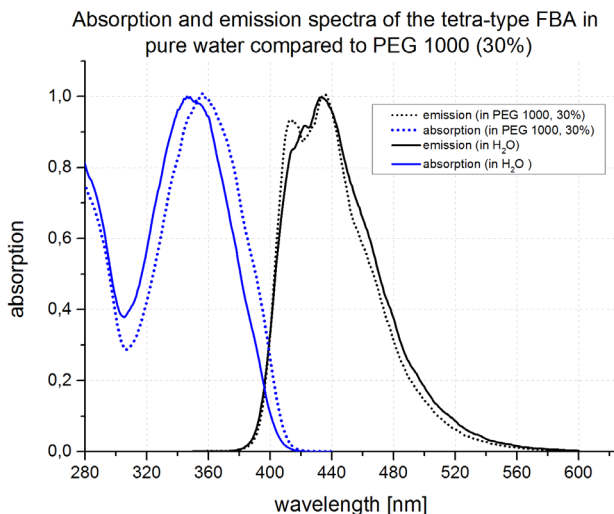


*Figure 18: Absorption and emission spectra of the tetra-based FBA once solved in pure water and once in 30% PEG 1000*

## Discussion

The presented results show that the quantum yield of commercially available FBAs can be increased by the addition of carrier substances. Thereby, it was found that the obtainable quantum yield directly correlates with the actual chain-length of used carrier-molecules.

The correlation between chain length and emission intensity was also found empirically for printed FBA-ink-layers on unbrightened.

Figure 19 shows the obtained emission spectra of FBA-ink samples printed on the unbrightened substrate „Epson SPP 205“. With Figure 16 and Figure 17 in mind, it can be concluded that the obtained second peak at 415nm for the 5%-PEG, 6.4%-tetra-type FBA-ink result out of a higher ratio of the trans-isomer. Hence, PEG-chain-length related effects do not only occur while in the liquid state and detached from the molecular environment “paper” but also in the non-liquid state, e.g. if applied using inkjet or applied during paper-production.

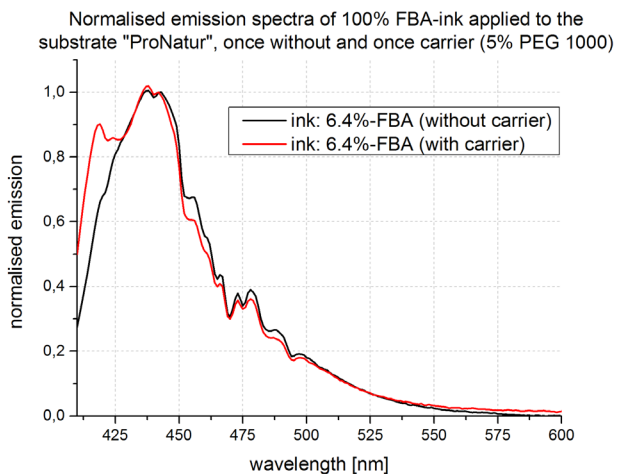


**Figure 19:** Normalised emission spectra of 100% FBA-ink applied to the substrate "ProNatur", once without and once carrier (5% PEG 1000). A blue-shift is found for the carrier containing sample

Against this background, the theories of Paltakari and Blum seem to be unlikely:

- Blume assumed that carriers promote a monomolecular distribution of FBAs in one layer on a paper-surface. Since in this study observed effects also occur while in the liquid state no monomolecular distribution can be realized.
- Paltakari suggested that FBAs and carriers create "some kind of complex". Out of a chemical perspective, a complex is typically related to metal components. This is very unlikely for the given substances. Anyhow, in this study it is assumed, that long-chained PEGs are linked together for high concentrations, intensifying this way the steric hindering of the C=C double bond. This can be interpreted as some kind of complex.

## Conclusions

In this study it is shown, that the chain-length of carriers such as PEG has a very significant impact on the quantum yield. Already low concentrations (10%) of PEG in the liquid state, result in a boost from 33% quantum yield up to 60% (in the case of the tetra-type FBA). Anyhow, the actual chain-length of the carrier (derived from the actual average molar mass) is the driving factor for increased quantum yields. Spectral analysis indicate that this increase in quantum yield results mainly from higher numbers of trans-isomers compared to the number of cis-isomers (cis-trans ratio). It is shown, that this shifted ratio towards the trans-isomer results probable not only from viscosity related effects on the quantum yield but especially the chain length of the molecules, which can be interpreted as a substance specific parameter as it is considered by the FÖRSTER-HOFFMANN law. One possible explanation is that the chains lead to a certain "physical" hindering of the isomerization. This



effect is possibly intensified due to in one another cross-linked chains, increasing the physical boundary of the C=C double bond twist of the isomerization and thus reduces the reaction speed of the isomerization itself.

### Selected Bibliography

1. Abrash, S., Repinec, S. and Hochstrasser, R. M. 1990 “The Viscosity Dependence And Reaction Coordinate For Isomerization Of Cis-Stilbene.”, *Journal of Chemical Physics*, 93:1041–1053, DOI: 10.1063/1.459168
2. Beale, R. N. and Roe, E. M. F. 1953 “Ultra-violet absorption spectra of trans- and cis-stilbenes and their derivatives. Part I. trans- and cis-Stilbenes”, *J. Chem. Soc.*, DOI: 10.1039/JR9530002755
3. Blum, T., Linhart, F. and Frenzel, S. 2002 „Verfahren zur Herstellung von beschichtetem Papier mit hoher Weiße“, patent-number: EP 1 419 298 B1
4. Bohn, D., Dattner, M., Fehmer, S. and Urban, P. 2016 “A method to compensate fluorescence induced white point differences in proof-processes by printing liquid fluorescent brightening agents using inkjet”, in Enlund, N. and Lovreček, M. (eds), *Journal of Print and Media Technology Research*, Darmstadt.
5. Champ, S., Linhart, F., Kaub, H.P., Blum, T. and Nord, S. 2003, “Verstärkung der Wirkung von optischen Aufhellern mit Hilfe von Polymeren“, patent-number: WO 2003020808 A1, date of publication: 13. März 2003
6. Gispert, J.R. 2008 “Coordination Chemistry”, (Wiley-VCH), p. 483. ISBN: 3-527-31802-X.
7. Holik, H. 2006, „Handbook of paper and board“, (Wiley-VCH, Weinheim) ISBN: 3527608338
8. Kasha, M., 1950, “Characterization of Electronic Transitions in Complex Molecules”, *Discussions of the Faraday Society*, p.14-19.
9. Horiba, UK Limited 2017 “Quantum Yield Standard”, Last accessed 03.19.2017, <http://www.horiba.com/fileadmin/uploads/Scientific/Documents/Fluorescence/quantumyieldstrad.pdf>
10. Knittel, T., Fischer G. and Fischer E. 1974 “Temperature dependence of Photoisomerization. Part VIII. Excited-State Behavior of 1-Naphthyl-2-Phenyl- And 1,2-Dinaphthyl-Ethylenes and Their Photocyclisation Products, And Properties Of The Latter.”, *J. Chem. Soc. Perkin Trans. 2*, DOI: 10.1039/P29740001930.

11. Paltakari, J. 2009 “Pigment coating and surface sizing of paper”, (2nd edn, Paperi ja Puu Oy, Helsinki)
12. Sauer, M., Hofkens, J. and Enderlein, J. 2011 “Handbook of fluorescence spectroscopy and imaging. From single molecules to ensembles” Wiley-VCH (Weinheim)
13. Schmidt-Weber, P., 2008 „Functionalisation of Surfaces“, Ph.d. thesis, FU Berlin, Berlin
14. Todd, D.C, Jean, J. M., Rosenthal, S. J., Ruggiero, A. J., and Yang, D. 1990, The Journal of Chemical Physics 93, 8658, doi: <http://dx.doi.org/10.1063/1.459252>